

NMSSM explanations of the Galactic center gamma ray excess and promising LHC searches

Jun Guo¹, Jinmian Li², Tianjun Li^{1,3} and Anthony G. Williams²

¹ *State Key Laboratory of Theoretical Physics, Institute of Theoretical Physics,
Chinese Academy of Sciences, Beijing 100190, P. R. China*

² *ARC Centre of Excellence for Particle Physics at the Terascale,
Department of Physics, University of Adelaide, Adelaide, SA 5005, Australia*

³ *School of Physical Electronics, University of Electronic Science
and Technology of China, Chengdu 610054, P. R. China*

The Galactic Center Excess (GCE) is explained in the framework of the Next-to-Minimal Supersymmetric Standard Model (NMSSM) with a Z_3 discrete symmetry. We show that a resonant CP-odd Higgs boson with mass twice that of the Dark Matter (DM) candidate is favoured. Meanwhile, the DM candidate is required to have relatively large coupling with the Z boson through its Higgsino component in order to obtain correct DM relic density. Its LHC discovery potential via four signatures is discussed in detail. We find that the most sensitive signals are provided by the Higgsino-like chargino and neutralino pair production with their subsequent decays into W bosons, Z bosons, and DM. The majority of the relevant parameter space can be probed at the Large Hadron Collider with a centre-of-mass energy of 14 TeV and an integrated luminosity 1000 fb^{-1} .

I. INTRODUCTION

The only current empirical evidence for the existence of Dark Matter (DM) is from gravitational effects, for example, the rotation curves of spiral galaxies and studies of mass distributions through gravitational lensing. However, it seems reasonable to expect that DM may have a common origin with Standard Model (SM) matter since the ratio of the relic density of DM to the relic density of SM matter is approximately 5 to 1, i.e., a number of order one. If the DM and SM origins were unrelated, then there would be no reason to expect this to occur. If there is a common origin, perhaps in some Grand Unified Theory (GUT), then it seems reasonable to expect that there may be some non-gravitational interactions between DM and SM matter as well. There is however no clear and broadly accepted evidence for such interactions to date. In particular, the absence of any convincing signals in spin independent DM direct detection experiments [1, 2] has already imposed very stringent upper limits on the couplings of DM particles to the SM particles.

DM can also be searched for through indirect signals arising from DM-DM annihilation into

SM particles in regions of high DM density. Such decays would potentially lead to anomalies in the energy spectra of gamma rays, anti-protons, electrons, positrons and so on, where an anomaly would be something that could not be understood in terms of known astrophysical sources. A recent analysis of the Fermi Gamma-Ray Space Telescope data [3], has shown a significant excess of gamma rays from the Galactic Center (GC). This GC Excess (GCE) in the range of $\sim [1, 3]$ GeV can be fitted very well by a 31-40 GeV DM particle annihilating into $b\bar{b}$ with an annihilation cross section of $\langle\sigma v\rangle = (1.4 \sim 2.0) \times 10^{-26} \text{ cm}^3/\text{s}$, or a 7-10 GeV DM particle annihilating into $\tau\bar{\tau}$ with similar cross section. Potential explanations of the GCE have been studied extensively using both model-dependent and model-independent approaches [4–34].

It is well-known that supersymmetry (SUSY) provides a natural solution to the gauge hierarchy problem in the SM and, in addition, SUSY leads to improved gauge coupling unification. Furthermore, with the assumption of R -parity conservation the lightest supersymmetric particle (LSP) such as the neutralino is stable and so is a good cold DM candidate. In short, SUSY is one of the most promising candidates for new physics beyond the SM. However, the Minimal SSM (MSSM) is challenged by the discovery of the 125 GeV Higgs boson [35, 36] due to the so-called little hierarchy problem concerning the fine tuning at the electroweak scale. In the Next-to-MSSM (NMSSM) [37], the SM-like Higgs boson mass can be lifted by both tree-level coupling and the mixing with a lighter singlet [38–48]. Thus, one can naturally obtain a relatively heavy Higgs boson. Moreover, the NMSSM has the advantage of also solving the μ problem in the MSSM, where the electroweak scale μ can naturally be generated by a singlet vacuum expectation value (VEV) at $\mathcal{O}(100)$ GeV. In this paper, we demonstrate another merit of the NMSSM, which is the potential to explain the GCE elegantly through a light singlet-like CP-odd Higgs.

Several studies of the GCE have been undertaken in the context of the NMSSM. DM pairs can annihilate into $b\bar{b}$ or $\tau\bar{\tau}$ via t-channel bottom squark or tau slepton exchange [18]. This process is, however, highly constrained by sparticles searches at LEP and LHC, by SM precision measurements as well as by DM direct detection searches. If the singlet-like scalar/pseudoscalar in the NMSSM is lighter than the DM particle, the DM pair annihilating into those new Higgs bosons that in turn have a dominant decay into bottom quarks [12, 49] will be able to give a promising fit to the gamma ray spectrum. This explanation requires an appropriate relationship between the final state Higgs boson mass and its coupling to DM and this can typically be realized within the general NMSSM framework. However, in the Z_3 NMSSM we find that the DM mass, the singlet scalar/pseudoscalar mass and their couplings are correlated and so there is less freedom to achieve this. We will briefly illustrate these difficulties concerning the Z_3 NMSSM later. A more promising channel is the

s -channel pseudoscalar mediated annihilation [19, 22, 28]. The annihilation cross section of this process can receive a Breit-Wigner enhancement when the pseudoscalar mass is approximately twice the DM mass where the resulting process is not suppressed by small DM velocity. We will focus on this scenario in this work [88]. A right-hand sneutrino DM particle in the NMSSM can also provide a possible explanation of the GCE through its annihilation into bottom quark pair [50] or CP-even/CP-odd Higgs bosons pair [51], while fulfilling other experimental constraints, however these studies are considerably more involved and we will not consider them further in this work.

The CERN Large Hadron Collider (LHC) is vigorously continuing its searches for evidence of SUSY. The current searches have the ability to exclude electroweakinos with masses below ~ 700 GeV [52]. The next run of LHC at a centre-of-mass energy of 14 TeV will start in 2015. If SUSY is not found in this next run, then it will provide much higher lower-mass bounds on all SUSY particles. Thus, whether or not we can probe the above NMSSM scenario at the 14 TeV LHC is an interesting question. On the one hand, DM is expected to have relatively large annihilation cross section to SM particles in order to reproduce both the correct DM relic density and the GCE. Hence, the inverse process may help to produce significant numbers of DM pairs at the LHC if the DM mass is not too large. On the other hand, the GCE scenarios in the NMSSM generically have light Higgsinos as well. So, probing the existence of a relatively light Higgsino can become a smoking gun for an explanation of the GCE in the NMSSM. We conclude that it will be difficult to search for the direct DM pair production with a mono-jet signature, whereas most of the viable parameter space is discoverable at 14 TeV LHC with 1000 fb^{-1} of data by searching for $WZ + \text{DM}$ final states decaying from Higgsinos.

This paper is organised as follows. In Section II, based on the analysis in Ref. [3], we briefly introduce the gamma ray flux measurement at the galactic centre. We study in detail the accommodation of the GCE in the NMSSM in Section III. In Section IV, we discuss some potential signatures and the discovery potential of the s -channel A_1 mediated annihilation scenario at the LHC. In particular, we investigate the required data sample necessary to fully explore the viable parameter space. Finally, we summarize and present our conclusion in Section V.

II. DARK MATTER ANNIHILATION AND GCE

Indirect detection, which focuses on DM annihilation into SM particle final states, is an important method to search for non-gravitational evidence of DM. The galactic centre is expected to have a relatively large DM number density due to gravitational effects and so is the most promising place

for dark matter indirect detection. Gamma ray signals of DM annihilation have advantages over the other indirect searches such as those involving anti-protons, positrons, and electrons, as gamma rays are neither deflected by magnetic fields nor do they lose energy during their propagation.

The gamma-ray flux produced from DM annihilation near the galactic centre and then detected near the Earth is given by

$$\frac{d\Phi}{dE_\gamma} = \frac{1}{4\pi} \frac{\langle\sigma v\rangle}{2m_{DM}^2} \frac{dN_\gamma}{dE_\gamma} \int_{\Delta\Omega} \langle J \rangle d\Omega' , \quad (1)$$

where

$$\langle J \rangle = \int_{\text{los}} \rho^2(\mathbf{r}) dl \quad (2)$$

is the so-called J-factor which encapsulates the dark matter distribution integrated over a solid angle $\Delta\Omega$ along the line-of-sight (los) and where dN_γ/dE_γ is the gamma-ray spectrum dependent on the properties of the final states of the DM annihilation and their kinematical features. Here, $\rho(\mathbf{r})$ is the assumed density distribution of the galactic DM halo.

The Milky Way's DM density distribution is assumed to be approximately spherically symmetric and hence can be approximately described as a function $\rho(r)$ of distance r from the Galactic Center. The NFW (Einasto and Navarro, Frenk and White) profile [53, 54] provides good fits to DM numerical simulations and is given by

$$\rho(r) = \rho_0 \left(\frac{r}{r_s}\right)^{-\gamma} \left[1 + \left(\frac{r}{r_s}\right)\right]^{\gamma-3} , \quad (3)$$

where the scale parameter r_s , the density parameter ρ_0 and the central slope parameter γ characterise the DM halo. The canonical NFW value of the central slope parameter is $\gamma = 1$. We follow Ref [3] who use a scale parameter of $r_s = 20$ kpc and choose ρ_0 so as to give a dark matter density around the Sun of $\rho(r_{\text{sun}}) = 0.3 \text{ GeV cm}^{-3}$, where the distance of the Sun from the Galactic Centre is $r_{\text{sun}} = 8.5$ kpc. This reference allows γ to be a free parameter and obtains a best fit value of $\gamma = 1.26$. For those DM indirect detections which focus on the Galactic Center the uncertainty of $\rho^2(r)$ can become extremely large very close to the center.

The J-factor can be rewritten as follows

$$J = \int db \int dl \int ds \cos b \rho(r)^2 , \quad (4)$$

in which $r = (s^2 + r_s^2 - 2sr_s \cos l \cos b)^{1/2}$ is the Galactocentric distance, and (l, b) are respectively the longitude and latitude angles. Ref. [3] considered the gamma spectra within a $5^\circ \times 5^\circ$ region around Galactic Center. s is the line of sight distance which has to be integrated over.

The last and most important factor, the annihilation cross section $\langle\sigma v\rangle$, affects both indirect detection and DM relic density predictions, is a model dependent variable. The relic density is approximately given by

$$\Omega h^2 = \frac{m_\chi n_\chi}{\rho_c} \simeq \frac{3 \times 10^{-27} \text{cm}^3 \text{s}^{-1}}{\langle\sigma v\rangle}. \quad (5)$$

At the freeze-out $v \sim 0.1$, one usually needs an annihilation cross section around 1 pb to produce the correct relic density $\Omega h^2 \simeq 0.1$ [55]. The analysis of Ref [3] showed that if the DM annihilates only into $b\bar{b}$ final states with $v \sim 10^{-3}$, one would need $\langle\sigma v\rangle \simeq 2.2 \times 10^{-26} \text{cm}^3 \text{s}^{-1}$ to produce the observed Gamma Ray Excess. Surprisingly, such annihilation cross sections can almost lead to the observed relic density. In the non-relativistic limit, the annihilation cross section can be written as $\langle\sigma v\rangle = a + \mathcal{O}(bv^2)$. If a single process is used to explain the relic density and GCE simultaneously, the a term should be non-vanishing and dominate the $\langle\sigma v\rangle$.

III. GCE IN THE NMSSM

In this Section, we will apply the Galactic Center gamma-ray Excess to a phenomenological NMSSM with a Z_3 discrete symmetry. The corresponding superpotential is [37]

$$W_{\text{NMSSM}} = h_u \hat{H}_u \hat{Q} \hat{U}_R^c + h_d \hat{H}_d \hat{Q} \hat{D}_R^c + h_e \hat{H}_d \hat{L} \hat{E}_R^c + \lambda \hat{S} \hat{H}_u \hat{H}_d + \frac{\kappa}{3} \hat{S}^3, \quad (6)$$

where \hat{Q} , \hat{U}_R^c , \hat{D}_R^c , \hat{L} , \hat{E}_R^c , \hat{H}_u , \hat{H}_d are the superfields for quark doublet, right-handed up-type quark, right-handed down-type quark, lepton doublet, right-handed charged lepton, up-type Higgs doublet, and down-type Higgs doublet respectively.

Because of the absence of sparticles with mass equal to their SM partners, SUSY has to be broken at a high energy scale in the hidden sector, and then the breaking effects are transmitted to the observable sector. The low energy supersymmetry breaking soft terms such as gaugino masses, scalar masses, and trilinear soft terms are

$$\begin{aligned} -\mathcal{L}_{\text{soft}} = & \frac{1}{2} \left(M_3 \tilde{g} \tilde{g} + M_2 \tilde{W} \tilde{W} + M_1 \tilde{B} \tilde{B} \right) \\ & + m_{H_u}^2 |H_u|^2 + m_{H_d}^2 |H_d|^2 + m_S^2 |S|^2 + m_Q^2 |Q|^2 + m_U^2 |U_R|^2 \\ & + m_D^2 |D_R|^2 + m_L^2 |L|^2 + m_E^2 |E_R|^2 \\ & + (h_u A_u Q H_u U_R^c - h_d A_d Q H_d D_R^c - h_e A_e L H_d E_R^c \\ & + \lambda A_\lambda H_u H_d S + \frac{1}{3} \kappa A_\kappa S^3 + h.c.) , \end{aligned} \quad (7)$$

where \tilde{g} , \tilde{W} , and \tilde{B} are gluino, Wino, and Bino respectively.

The NMSSM has five neutralinos ($\tilde{\chi}_i^0$), which are the mass eigenstates of mixings among $\tilde{B}, \tilde{W}, \tilde{H}_d^0, \tilde{H}_u^0$, and \tilde{S} . Following the convention of Ref. [37], we give the mass matrix for the neutralino sector in Appendix A. Because of the extra singlet in the NMSSM, the neutral Higgs sector is also expanded. There are 3 CP-even Higgs (H_i) and 2 CP-odd Higgs (A_i), both of which are mixed among H_d, H_u and S gauge eigenstates. We find it more convenient to discuss the CP-even and CP-odd Higgs mass matrixes in the Goldstone basis [56], $S_i, (i = 1, 2, 3)$ and $P_i, (i = 1, 2)$. Their mass matrixes are presented in Appendix A as well for later discussion.

Now, we are ready to discuss the feasibility of the scenarios that could fulfil the observation of the Galactic Center Gamma-ray Excess in the NMSSM, while remaining consistent with other experimental results.

A. s -Channel A_1 Resonant Annihilation

As has been studied in Ref. [3], when DM annihilates directly into $b\bar{b}$, we need the DM to have mass $m_{\text{DM}} \sim 35$ GeV and $\langle\sigma v\rangle|_{v\rightarrow 0} \sim 2 \times 10^{-26}$ cm³/s to produce the observed GCE. Interestingly, the $b\bar{b}$ final state is commonly favoured due to its relatively larger Yukawa coupling if the s -channel annihilation is mediated by a relatively light Higgs boson. However, the Higgs boson mediator can not be CP-even primarily because of the following two reasons:

- Annihilation which is mediated by an s -channel CP-even Higgs is suppressed by small DM velocity. As discussed in Section II, in this case, the dark matter will annihilate much faster at early times than it does today. So $\langle\sigma v\rangle|_{v\rightarrow 0} \sim 2 \times 10^{-26}$ cm³/s will lead to a very small relic density; and
- The CP-even Higgs boson can also mediate spin-independent DM interactions with SM matter and give a direct detection signal, which has a current bound as low as 10^{-9} pb [1]. This makes it very difficult to achieve a signal consistent with the GCE while satisfying the direct detection constraints.

In principle, the CP-odd Higgs boson can be a very good s -channel mediator candidate. Firstly, there is no velocity suppression in its annihilation. A fermion-antifermion pair with momentum [57]

$$k_1^\mu = (E_1, \vec{k}) = (\sqrt{m_{\text{DM}}^2 + \vec{k}^2}, \vec{k}), \quad (8)$$

$$k_2^\mu = (E_2, -\vec{k}) = (\sqrt{m_{\text{DM}}^2 + \vec{k}^2}, -\vec{k}), \quad (9)$$

have the corresponding spinors

$$u(k_1) = \begin{pmatrix} \frac{k_1 \cdot \sigma + m_{DM}}{\sqrt{2(k_1^0 + m_{DM})}} \zeta_1 & \frac{k_1 \cdot \bar{\sigma} + m_{DM}}{\sqrt{2(k_1^0 + m_{DM})}} \zeta_1 \end{pmatrix}^T, \quad (10)$$

$$v(k_2) = \begin{pmatrix} \frac{k_2 \cdot \sigma + m_{DM}}{\sqrt{2(k_2^0 + m_{DM})}} \zeta_2 & \frac{k_2 \cdot \bar{\sigma} + m_{DM}}{\sqrt{2(k_2^0 + m_{DM})}} \zeta_2 \end{pmatrix}^T. \quad (11)$$

The matrix element of dark matter annihilation with a pseudoscalar vertex $\bar{u}\gamma^5 v A$ is

$$\bar{u}\gamma^5 v = -\frac{1}{\sqrt{(E_1 + m_{DM})(E_2 + m_{DM})}} [(E_1 + m_{DM})(E_2 + m_{DM}) + \vec{k}^2] (\zeta_1^\dagger \zeta_2), \quad (12)$$

where the first term is dominant and does not suffer from any velocity suppression.

Secondly, the interaction of DM and nucleon through t -channel CP-odd Higgs is spin dependent. For the same vertex $\bar{u}\gamma^5 u A$ the matrix element of the direct detection process is

$$\begin{aligned} \bar{u}(p_1)\gamma^5 u(p_2) &= \frac{1}{\sqrt{(p_1^0 + m_{DM})(p_2^0 + m_{DM})}} \xi_1^\dagger [(p_2^0 + m_{DM})(\vec{p}_1 \cdot \vec{\sigma}) - (p_1^0 + m_{DM})(\vec{p}_2 \cdot \vec{\sigma})] \\ &\sim 2(p_1 - p_2)^i (\xi_1^\dagger \hat{S}^i \xi_2), \end{aligned} \quad (13)$$

which only gives a spin-dependent amplitude. So, the stringent bound from spin-independent direct detection experimental searches does not apply.

However, in a realistic NMSSM treatment, there are additional constraints that should be considered. In order to have a relatively large DM annihilation cross section, the CP-odd Higgs boson can not be too heavy. Also, its couplings to the SM particles should be suppressed to evade the current collider searches. Interestingly, a light singlet-like CP-odd Higgs (A_1) can meet the need. As a result, we will assume a light singlet superfield in our model. Also, it is natural to require that our DM be singlino dominant [89]. Its mass is approximately $m_{\tilde{\chi}_1^0} \sim 2\kappa s$, which means

$$\frac{\kappa}{\lambda} = \frac{m_{\tilde{\chi}_1^0}}{2\mu_{\text{eff}}} \lesssim \frac{35}{200}, \quad (14)$$

where the second inequality is from the non-discovery of any chargino at the LEP experiment [58]. The requirement of having no Landau pole all of the way up to the GUT scale imposes the requirement that

$$\sqrt{\lambda^2 + \kappa^2} \lesssim 0.5, \quad (15)$$

which indicates that κ can only be $\lesssim 0.1$. The requirement of A_1 being singlet-like leads to a suppression of the $A_1 b\bar{b}$ coupling, although it might be enhanced with the choice of a relatively large $\tan\beta$. So both vertexes of $A_1 b\bar{b}$ and $A_1 \tilde{\chi}_1^0 \tilde{\chi}_1^0$ are suppressed and typically it is not possible to get the correct right relic density as well as a signal consistent with the GCE with such small

couplings. However, a resonant enhancement can resolve this problem: when the total invariant mass of the initial states is close to the A_1 mass, the total annihilation cross section is enhanced by a Breit-Wigner factor

$$R(s) = \frac{1}{(s - M_A^2)^2 + \Gamma_A^2 M_A^2}. \quad (16)$$

The cross section of such process is given by

$$\langle\sigma v\rangle = \frac{3}{8\pi} \sqrt{1 - \frac{m_b^2}{m_{\tilde{\chi}_1^0}^2} \frac{\kappa^2 C_{A_1 d} m_b^4 \tan^2 \beta}{(s - m_{A_1}^2)^2 + \Gamma_{A_1}^2 m_{A_1}^2}}. \quad (17)$$

Thus, we need to require the mass of the CP-odd Higgs A_1 to be approximately 70 GeV to reproduce the GCE signal. A problem still exists if we want to accommodate the relic density simultaneously. At the early stage of the Universe when DM is frozen out, the temperature of the Universe is around $m_{\tilde{\chi}_1^0}/20$ [59]. So, the energy of the DM is slightly higher at freeze-out than today. The Breit-Wigner factor is very sensitive to the initial energy around the mediator mass. The $\langle\sigma v\rangle|_{v\rightarrow 0} \sim 2 \times 10^{-26}$ cm³/s today will lead to an over abundance of relic DM because of the reduction of resonant enhancement. To resolve this we can increase the annihilation cross section at freeze-out by including a small Higgsino component in the DM, which will give an additional contribution from the s -channel Z boson exchange. From Eqs. (45) and (46), we need small μ to get relatively large Higgsino components in DM. Moreover, the coupling between DM and the Z boson is proportional to $\tan\beta$. So, a relatively large $\tan\beta$ is required in our model as well. As will be shown numerically later, a $Z\tilde{\chi}_1^0\tilde{\chi}_1^0$ coupling that can give the correct DM relic density can still be consistent with the constraints on Z boson invisible decays. The coupling between the DM and Higgs boson is enhanced by large λ and, furthermore, the \tilde{H}_d component in DM is increased by large $\tan\beta$. So H_{SM} may have considerable decay branching ratio to DM in this scenario.

Following the above arguments, we have found a viable DM scenario which can explain the relic density and GCE, and is consistent with DM direct searches. Similar scenarios for singlino/Higgsino mixing DM have been studied in [22]. In their analysis, however, some experimental constraints, such as constraints on Higgs invisible decay, are overlooked. We will present a concrete model below which satisfies all of the current experimental constraints. Moreover, we have different conclusions regarding the Bino/Higgsino mixing case and, as we will comment on later, the resonant DM annihilation enhancement can still be applied. Before we present our the numerical scan, let us study the parameter space more carefully to understand the correlations among the NMSSM parameters.

The singlet tends to be lighter than the SM Higgs boson. Since the measurements of H_{SM} are likely to be consistent with the SM couplings, the mixing between the H_u/H_d doublets and singlet should be suppressed in most cases. So we can arrive at an approximate value for A_λ , as shown in Eq. (49). Also, in the CP-even Higgs matrix, the M_A^2 is enhanced by a factor of $1/\sin^2 2\beta$, which will increase greatly with large $\tan\beta$. So, we can safely decouple S_1 component in the CP-even Higgs matrix and the P_1 component in the CP-odd Higgs matrix in the following discussions. Then from the CP-odd Higgs boson mass matrix in Eq. (50) we obtain

$$M_{A_1}^2 \simeq -3A_\kappa \frac{\kappa\mu}{\lambda} + \frac{\lambda^2 v^2}{2\mu} s_{2\beta} \left(A_\lambda + \frac{4\kappa\mu}{\lambda} \right) \simeq -3A_\kappa \frac{m_{\tilde{\chi}_1^0}}{2} + \lambda^2 v^2 \left(1 + \frac{\sin 2\beta m_{\tilde{\chi}_1^0}}{2\mu} \right), \quad (18)$$

where we have substituted Eq. (49) and $m_{\tilde{\chi}_1^0} \sim 2\kappa s$. Note that when $m_{\tilde{\chi}_1^0} \sim 35$ GeV, $\mu \gtrsim 100$ GeV, and $\tan\beta$ is large, the second term in the bracket of Eq. (18) can be ignored. As a result, A_κ is approximately fixed to the value

$$A_\kappa = \frac{2(\lambda^2 v^2 - M_{A_1}^2)}{3m_{\tilde{\chi}_1^0}}. \quad (19)$$

Another possible problem is the Higgs invisible decay. Although the direct bound on the SM-like Higgs invisible decay is still very weak, $\text{Br}(H_{\text{inv}}) \lesssim 75\%$ [60], the current Higgs coupling measurement requires that the Higgs signal strength to the SM particles be around 1. Because in most of our models, there is no additional Higgs production mechanism, the Higgs invisible decay branching ratio is thus highly constrained indirectly. The main contribution to the vertex $H_2 \tilde{\chi}_1^0 \tilde{\chi}_1^0$ is the superpotential term $W = \lambda S H_u H_d$ and the corresponding coupling for $H_2 \tilde{\chi}_1^0 \tilde{\chi}_1^0$ is proportional to $C_{\tilde{\chi}_1^0 d} \frac{\lambda}{\sqrt{2}}$, where $C_{\tilde{\chi}_1^0 d}$ is the \tilde{H}_d component in the DM $\tilde{\chi}_1^0$. Hence we find

$$\Gamma_{H_2 \rightarrow \tilde{\chi}_1^0 \tilde{\chi}_1^0} = \frac{(1/4 m_{H_2}^2 - m_{\tilde{\chi}_1^0}^2)^{\frac{3}{2}}}{\pi m_{H_2}^2} \times \lambda^2 C_{\tilde{\chi}_1^0 d}^2. \quad (20)$$

Thus, the Higgs invisible decay is enhanced by large λ and $C_{\tilde{\chi}_1^0 d}$.

Let us summarize the results that we have so far:

- The s -channel mediator of DM annihilation should be a singlet-like CP-odd Higgs boson, whose mass is around $2 \times m_{\text{DM}}$. This will fix the A_κ parameter;
- The singlino dominant DM should have a small Higgsino component, which requires a small μ and large $\tan\beta$. Interestingly, natural SUSY requires a small μ as well;
- The purity of the H_{SM} can be fulfilled by setting an appropriate A_λ ; and
- The Higgs invisible decay limit needs to be carefully accounted for.

We use the NMSSMtools [61–63] software to survey the viable parameter space in the NMSSM at the electroweak scale. The DM relic density and the DM direct and indirect detection rates are calculated using micrOMEGAs [64–66]. We apply the following constraints implicitly for our study:

- Theoretical constraints including converged RGE running, no tachyons, no Landau pole below the GUT scale, a physical global minimal and so on;
- Limits from the Higgs and sparticle searches at the LEP and Tevatron experiments;
- B physics constraints;
- Limits on the Z boson invisible decay width;
- The SM Higgs mass lies in the range of [123, 128] GeV and its signal strengths for all channels are lies in range of [0.8, 1.2] of the SM values; and
- The requirement of a good dark matter candidate that has the properties $0.09 < \Omega h^2 < 0.12$, $\sigma_{\text{SI}} < 1 \times 10^{-9}$ pb, and $0.5 \times 10^{-26} \text{cm}^3/s < \langle \sigma v \rangle < 5 \times 10^{-26} \text{cm}^3/s$.

Within the scenario that we have proposed, to further simplify our scanning, we decouple the irrelevant sparticles by choosing

$$\begin{aligned}
 M_1 &= 1 \text{ TeV}, M_2 = 2 \text{ TeV}, M_3 = 3 \text{ TeV}, m_L = m_E = 1 \text{ TeV} , \\
 A_e &= 0 \text{ TeV}, m_{Q_2} = 2 \text{ TeV}, m_{Q_3} = 1.5 \text{ TeV}, m_{U_2} = m_{D_2} = 3 \text{ TeV} , \\
 m_{U_3} &= 1.5 \text{ TeV}, m_{D_3} = 2.5 \text{ TeV}, A_b = 0 \text{ TeV} .
 \end{aligned} \tag{21}$$

We scan the remaining parameters in the following ranges

$$\begin{aligned}
 \lambda &: [0.35, 0.65], \quad \kappa : [30, 45] \times \frac{\lambda}{2\mu}, \quad \tan \beta : [10, 40] , \\
 \mu &: [100, 600] \text{ GeV}, \quad A_\kappa : [-100, 100] \text{ GeV} , \\
 A_\lambda &= 2\mu / \sin 2\beta - 2\kappa\mu / \lambda, \quad A_t = \mu / \tan \beta + \sqrt{6} \times 1500 .
 \end{aligned} \tag{22}$$

Our numerical results are shown in Fig. 1. The DM annihilation today is greatly enhanced by the A_1 resonance, especially in the region $m_{A_1}/2m_{\tilde{\chi}_1^0} \gtrsim 0.98$. However, the relic density is relatively large in the resonant region $m_{A_1}/2m_{\tilde{\chi}_1^0} \rightarrow 1$, which is mainly because of the reduced Breit-Wigner factor due to the large DM energy at freezing out.

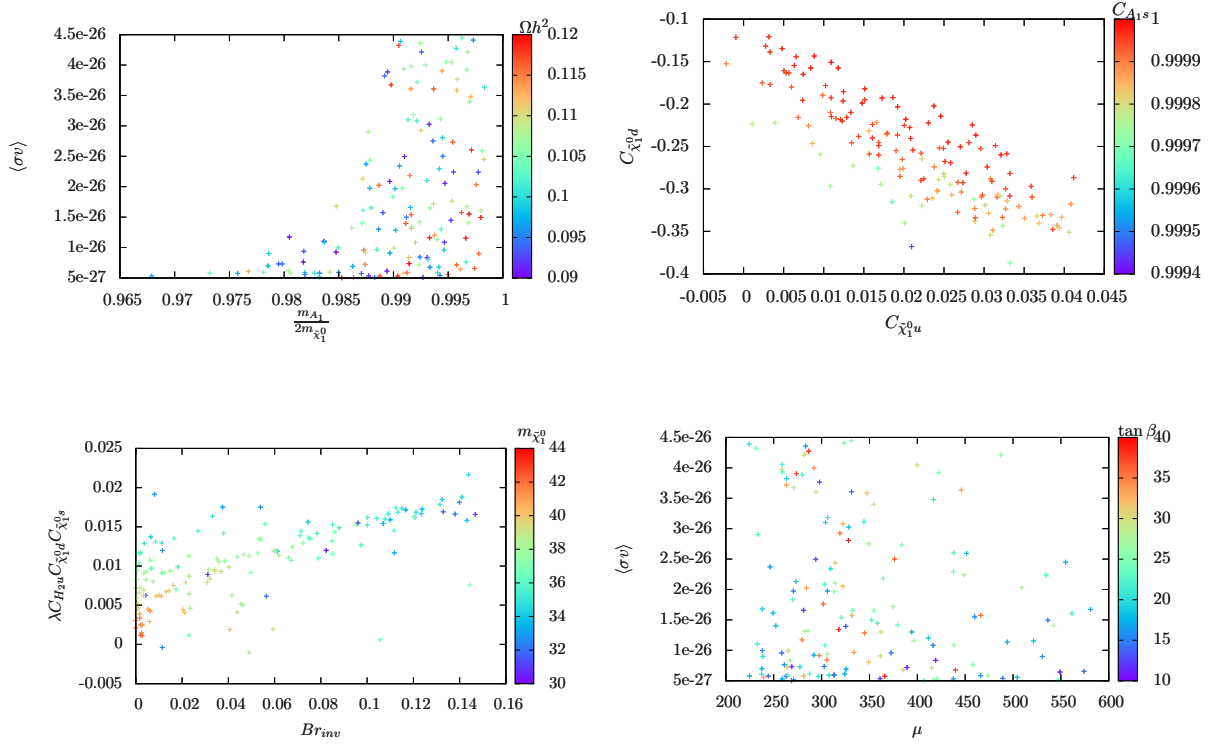


FIG. 1: All the points in figures satisfy the constraints that mentioned in the Section III. The corresponding x -axis and y -axis as well as color coding are given in each panel.

From the upper right panel of Fig. 1, we conclude that the annihilation of DM is still dominated by the κ coupling for $A_1 \tilde{\chi}_1^0 \tilde{\chi}_1^0$, even though the κ is preferably more than one order of magnitude smaller than λ

$$\lambda C_{\tilde{\chi}_1^0, d} C_{\tilde{\chi}_1^0, d} C_{A_1, s} \ll \kappa C_{\tilde{\chi}_1^0, s}^2 C_{A_1, s} . \quad (23)$$

From the figure, we also find that the coupling between the A_1 and the bottom quarks is indeed suppressed by its small H_d component.

On the other hand, the invisible decay of the SM-like Higgs boson H_{SM} is dominated by the large λ coupling, as shown in the lower left panel of Fig. 1. Thus, we need the smallness of \tilde{H}_d component in $\tilde{\chi}_1^0$ to suppress the coupling between the dark matter and SM-like Higgs boson. Note that because of Eq. (14), DM mass will decrease when increasing λ . The smaller Higgs invisible decay branching ratio usually means the heavier dark matter mass.

As we have emphasized before, the Higgsino component in the DM is very important to achieve the correct DM relic density. That is why one usually needs relatively small μ and large $\tan\beta$ in this scenario. As shown in the lower right panel of Fig. 1, we find μ preferably lies in the range

of [200, 600] GeV, which gives us a handle to discovery this scenario at the LHC, by searching for relatively light Higgsinos. We will present more extensive study in the next Section. Fig. 2 shows Higgsino-like neutralino decay branching ratios, in which both $\tilde{\chi}_2^0$ and $\tilde{\chi}_3^0$ have very large decay branching ratios to $Z\tilde{\chi}_1^0$ and $H_{\text{SM}}\tilde{\chi}_1^0$. And their decays to lighter Higgs bosons, which usually have branching ratios smaller than 10%, are suppressed by the large singlet component.

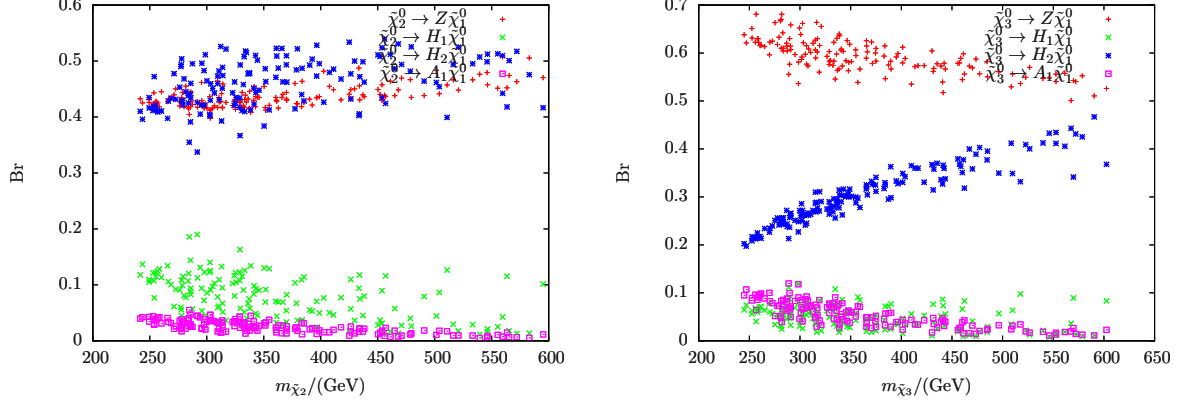


FIG. 2: All the points in figures satisfy the constraints that mentioned in the Section III. Left: Decay branching ratios for $\tilde{\chi}_2^0$. Right: Decay branching ratios for $\tilde{\chi}_3^0$.

In order to have a better understanding of this scenario, we present a benchmark point in Table I. From this table, the ratios of the DM annihilation into $b\bar{b}$ and e^+e^- at freeze out are quite

λ	κ	$\tan\beta$	μ	A_λ	A_κ
0.557	0.033	25.72	313.2	8029.5	9.51
A_t	m_{A_1}	m_{H_1}	m_{H_2}	$m_{\tilde{\chi}_1^0}$	$m_{\tilde{\chi}_2^0}$
3686.4	72.1	65.3	124.9	36.4	332.1
$m_{\tilde{\chi}_1^\pm}$	$\frac{\tilde{\chi}_1^0\tilde{\chi}_1^0 \rightarrow b\bar{b}}{\tilde{\chi}_1^0\tilde{\chi}_1^0 \rightarrow e^+e^-} _{\text{Freeze Out}}$	Ωh^2	$\langle\sigma v\rangle _{v\rightarrow 0}(\text{cm}^3/\text{s})$	$\sigma_{\text{SI}}(\text{cm}^2)$	$\text{Br}(H_2 \rightarrow \tilde{\chi}_1^0\tilde{\chi}_1^0)$
319.6	5.5	0.11	2.25×10^{-26}	6.34×10^{-50}	3.9%
$\text{Br}(\tilde{\chi}_2^0 \rightarrow Z\tilde{\chi}_1^0)$	$\text{Br}(\tilde{\chi}_2^0 \rightarrow H_2\tilde{\chi}_1^0)$	$\text{Br}(\tilde{\chi}_2^0 \rightarrow H_1\tilde{\chi}_1^0)$	$\text{Br}(\tilde{\chi}_3^0 \rightarrow Z\tilde{\chi}_1^0)$	$\text{Br}(\tilde{\chi}_3^0 \rightarrow H_2\tilde{\chi}_1^0)$	$\text{Br}(\tilde{\chi}_3^0 \rightarrow H_1\tilde{\chi}_1^0)$
41.8%	46.3 %	8.8%	59.7%	28.7%	5.4%

TABLE I: The benchmark point for s -Channel A1-resonant annihilation, which satisfies all the constraints mentioned in the text and whose other soft parameters are given in Eq. (21). All mass parameters are in units of GeV.

similar to the decay branching ratios of Z boson. So we conclude that the DM annihilations are indeed dominated by the Z boson exchange in the early universe, while in the present universe the Z boson contributions suffer from both p -wave suppression and from being away from resonance pole. For this benchmark point, 90% of the DM annihilates into $b\bar{b}$. Following the same analysis as

in Ref. [3], we calculate the gamma ray spectrum for this benchmark point by using micrOMEGAs, which is given in Fig. 3. Thus, it can fit the observed GCE very well.

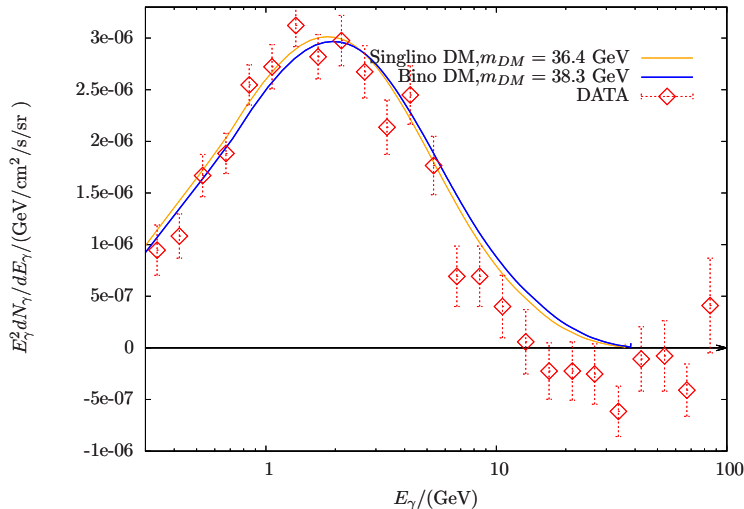


FIG. 3: The gamma-ray spectra of two benchmark points in Tables I and II. The generalised NFW halo profile with an inner slope of $\gamma = 1.26$ is chosen. And the angle distance from the Galactic Center is 5° .

Finally, let us briefly discuss the scenario where the DM is Bino dominant. In this case there is no constraint on the singlino mass so that κ becomes a free parameter and so there is not much difference between this and the singlino LSP scenario. In order to annihilate Bino-dominated DM effectively, we still need the A_1 resonant enhancement. A relatively large Higgsino component is needed to realize the correct DM relic density as well. As a result, except for the singlet state, the rest of the model properties are quite similar to the above singlino LSP scenario. We give a benchmark point in Table II. For this benchmark point, because the singlet is heavy, the lightest CP-even Higgs boson is SM-like and its invisible decay to DM is dominated by gauge coupling. The lightest CP-odd Higgs boson is singlet-like, with its proper mass $m_{A_1} \sim 2 \times m_{\tilde{\chi}_1^0}$ achieved by tuning A_κ . Moreover, the light Higgsino states decay in a manner similar to that in the singlino LSP scenario, where the decays are dominated by $Z\tilde{\chi}_1^0$ and $H_{SM}\tilde{\chi}_1^0$ final states.

B. Hidden Sector Dark Matter in the NMSSM

In this subsection, we will briefly comment on another possible explanation of GCE within the Z_3 NMSSM, where DM with mass $m_{\tilde{\chi}_1^0} \sim 67$ GeV can predominantly annihilate into H_1 and A_1 . Both H_1 and A_1 are singlet-like while having small fractions of H_d component. Then H_1 and A_1 mainly decay into $b\bar{b}$ because of the relatively large bottom quark Yukawa coupling. In this case,

λ	κ	$\tan\beta$	μ	A_λ	A_κ
0.173	0.558	30.23	175.5	4220.2	0.56
A_t	m_{A_1}	m_{H_1}	M_1	$m_{\tilde{\chi}_1^0}$	$m_{\tilde{\chi}_2^0}$
3234.1	76.75	124.1	41.9	38.3	184.8
$m_{\tilde{\chi}_1^\pm}$	Ωh^2	$\langle\sigma v\rangle _{v\rightarrow 0}(\text{cm}^3/\text{s})$	$\sigma_{SI}(\text{cm}^2)$	$\text{Br}(H_1 \rightarrow \tilde{\chi}_1^0 \tilde{\chi}_1^0)$	$\text{Br}(A_1 \rightarrow b\bar{b})$
179.7	0.118	2.38×10^{-26}	3.84×10^{-46}	15%	90%
$\text{Br}(\tilde{\chi}_2^0 \rightarrow Z\tilde{\chi}_1^0)$	$\text{Br}(\tilde{\chi}_2^0 \rightarrow H_1\tilde{\chi}_1^0)$	$\text{Br}(\tilde{\chi}_2^0 \rightarrow A_1\tilde{\chi}_1^0)$	$\text{Br}(\tilde{\chi}_3^0 \rightarrow Z\tilde{\chi}_1^0)$	$\text{Br}(\tilde{\chi}_3^0 \rightarrow H_1\tilde{\chi}_1^0)$	$\text{Br}(\tilde{\chi}_3^0 \rightarrow A_1\tilde{\chi}_1^0)$
52.7%	45.8%	1.5%	90%	8.2%	1.8%

TABLE II: The benchmark point with Bino-like DM, which satisfies all the constraints mentioned in the text and whose other soft parameters are given in Eq. (21). All mass parameters are in units of GeV.

we can not employ the resonant enhancement. So, DM can only be singlet-like and a very large coupling of the singlet state κ is required. The singlet mass $m_\chi \simeq 2\frac{\kappa}{\lambda}\mu$ implies

$$\frac{\kappa}{\lambda} = \frac{m_{\tilde{\chi}_1^0}}{2\mu_{\text{eff}}} \lesssim \frac{67}{200} . \quad (24)$$

The DM direct detection experiments also give strong constraints on the DM-nucleon scattering cross section. The main contributions to direct detection come from H_1 and H_2 mediated t -channel processes:

$$\sigma_{SI} \simeq \frac{\kappa^2 \mu_{\tilde{\chi}_1^0 N}^2 m_N^2 f_N^2}{4\pi v^2} \left(\frac{C_{H1u}}{m_{H_1}^2} + \frac{C_{H2s}}{m_{H_2}^2} \right)^2 , \quad (25)$$

where $f_N = \sum_{q=u,d,s} f_{T_q} + \frac{2}{9}f_{T_G} \simeq 0.348 \pm 0.015$ [67], C_{H1u} and C_{H2s} are the H_u component in H_1 and singlet component in H_2 respectively. To obtain a small spin-independent cross section, σ_{SI} , it is necessary to have a quite small mixing between H_u^0 and S due to

$$C_{H1u}^2 \simeq \sigma_{SI} \frac{4\pi v^2 m_{H_1}^4}{0.1^2 f_N^2} \left(\frac{0.1}{\kappa} \right)^2 < 0.004 . \quad (26)$$

To suppress the singlet component in the SM-like H_2 , we use the condition $A_\lambda = 2\mu/\sin 2\beta - 2\kappa\mu/\lambda$. Moreover, from Eq. (24) and the Landau pole condition $\lambda^2 + \kappa^2 \lesssim 0.5$, we have

$$|\kappa| \lesssim \sqrt{\frac{1}{2} \left(\frac{m_{\tilde{\chi}_1^0}^2}{m_{\tilde{\chi}_1^0}^2 + 4\mu^2} \right)} . \quad (27)$$

On the other hand, the cross section of dark matter annihilation into H_1 and A_1 is expected to be

$$\langle\sigma v\rangle \simeq \frac{\kappa^4}{4\pi m_{\tilde{\chi}_1^0}^2} \frac{|\vec{P}_3|}{m_{\tilde{\chi}_1^0}} \left(\frac{4m_{\tilde{\chi}_1^0}^2 + m_{A_1}^2 - m_{H_1}^2}{4m_{\tilde{\chi}_1^0}^2 - m_{A_1}^2 - m_{H_1}^2} - \frac{m_{\tilde{\chi}_1^0}^2 - A_\kappa m_{\tilde{\chi}_1^0}}{4m_{\tilde{\chi}_1^0}^2 - m_{A_1}^2} \right)^2 , \quad (28)$$

in which $|\vec{P}_3| = \sqrt{E_{A_1}^2 - m_{A_1}^2}$, and $E_{A_1} = \sqrt{\frac{4m_\chi^2 + m_{A_1}^2 - m_{H_1}^2}{4m_\chi}}$. As a result, the annihilation cross section is highly constrained by Eq. (27).

Following the same strategy as above, we survey the parameter space in the low energy NMSSM. We choose the same irrelevant soft terms as Eq. (21) and the ranges for the DM related parameters as follows

$$\lambda : [0.35, 0.65], \quad \kappa : -[50, 100] \times \frac{\lambda}{2\mu}, \quad \tan \beta : [1, 40]$$

$$\mu : [100, 500] \text{ GeV}, \quad A_\kappa : [-100, 100] \text{ GeV} \quad (29)$$

$$A_\lambda = 2\mu/\sin 2\beta - 2\kappa\mu/\lambda, \quad A_t = \mu/\tan \beta + \sqrt{6} \times 1500,$$

where a negative κ is taken to reduce the SM-like Higgs invisible decay into $A_1 A_1$.

As shown in the left panel of Fig. 4, the LUX experiment constrains $|\kappa|$ to be no larger than 0.12. This will lead to the DM annihilation cross section smaller than $\sim 1.2 \times 10^{-26} \text{ cm}^3/s$. From the right panel of the figure, we conclude that there is no great tension between the DM density and DM annihilation rate. However, a heavier DM tends to have a relatively large annihilation rate because of large $|\kappa|$.

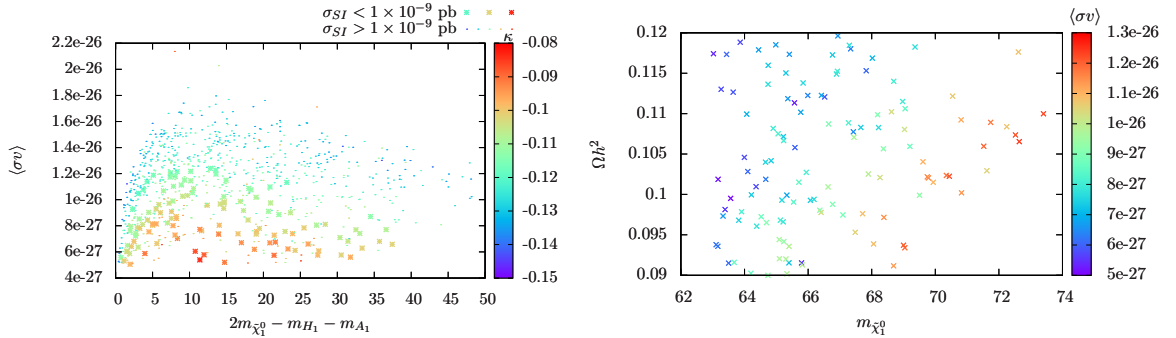


FIG. 4: Left: The recent direct detection LUX experiment gives a strong constraint. Because the larger κ means larger σ_{SI} , it is difficult to get a big $\langle\sigma v\rangle$ and $\langle\sigma v\rangle > 1.5 \times 10^{-26} \text{ cm}^3/s$ has been excluded by the LUX results. Right: All the points satisfy the constraints mentioned in the last two figures, so we can find an upper limit on $\langle\sigma v\rangle$.

We present a benchmark point for this scenario in Table III. This case usually has very small μ and relatively large $|\kappa|$. The spin-independent DM-nucleon cross section is close to the exclusion limit, while the annihilation cross section only reaches $1.22 \times 10^{-26} \text{ cm}^3/s$.

In short, the GCE in this scenario is constrained by the Landau pole condition and the DM direct search limits. It is difficult to have the DM annihilation cross section as large as expected,

λ	κ	$\tan\beta$	μ	A_λ	A_κ
0.374	-0.113	26.09	143.82	3846.26	39.716
A_t	m_{A_1}	m_{H_1}	m_{H_2}	$m_{\tilde{\chi}_1^0}$	$m_{\tilde{\chi}_2^0}$
3679.7	43.9	86.9	125.9	70.43	153.3
$m_{\tilde{\chi}_1^\pm}$	Ωh^2	$\langle\sigma v\rangle _{v\rightarrow 0}(\text{cm}^3/\text{s})$	$\sigma_{\text{SI}}(\text{cm}^2)$	$\text{Br}(H_2 \rightarrow A_1 A_1)$	$\text{Br}(H_1 \rightarrow b\bar{b})$
147.3	0.1026	1.22×10^{-26}	9.43×10^{-46}	4.5%	89.6%
$\text{Br}(\tilde{\chi}_2^0 \rightarrow Z\tilde{\chi}_1^0)$	$\text{Br}(\tilde{\chi}_2^0 \rightarrow H_2\tilde{\chi}_1^0)$	$\text{Br}(\tilde{\chi}_2^0 \rightarrow A_1\tilde{\chi}_1^0)$	$\text{Br}(\tilde{\chi}_3^0 \rightarrow Z\tilde{\chi}_1^0)$	$\text{Br}(\tilde{\chi}_3^0 \rightarrow H_2\tilde{\chi}_1^0)$	$\text{Br}(\tilde{\chi}_3^0 \rightarrow H_1\tilde{\chi}_1^0)$
0%	0 %	96.3%	62.3%	0%	29.96%

TABLE III: The benchmark point for hidden sector DM scenario. which satisfies all the constraints mentioned in the text. Also, the other soft parameters are given in Eq. (21). All mass parameters are in units of GeV.

$2.2 \times 10^{-26} \text{ cm}^3/\text{s}$. Nonetheless, the situation changes if we take into account the large uncertainty in background analysis [68, 69], where the allowed annihilation rate can vary in a large range $\sim [0.4, 4.5] \times 10^{-26} \text{ cm}^3/\text{s}$. We will not consider this case further in this work.

IV. DISCOVERY POTENTIAL AT THE LHC

We have shown that the s-channel A_1 mediated annihilation with singlino dominant DM is the most promising scenario and so we will restrict our attention to its discovery potential at the LHC. For this scenario, we have a light Higgs sector and a light singlino and Higgsino. The pseudoscalar, even though relatively light, is nearly pure singlet as shown in Fig. 1. So, it will be very difficult to produce it at the hadron collider. Moreover, we find it is very difficult to produce the pseudoscalar from the SM-like Higgs mediated processes and neutralino decays as well. The deviation of the coupling and invisible decay of the SM-like Higgs boson may also provide a smoking gun for this scenario. On the one hand, both the measurement accuracy of couplings that can be reached at the LHC [70] and the constraint on Higgs invisible decay [60] are very weak. On the other hand, and more importantly, the Higgs couplings and its invisible decay width vary in a large range in our scan, with many of the models having very SM-like couplings and suppressed invisible decay width, as indicated in Fig. 1. So, those signatures should not be able to provide very promising signals in the full parameter space of the scenario. However, in the electroweakino sector, there are two remarkable signatures for the viable NMSSM with GCE. The first one is that the DM particle has a relatively large Higgsino component and a moderately large coupling to the Z boson which guarantee the correct DM relic density. So, a natural thought will be the direct production of DM pair at the LHC through s -channel Z boson exchange. The second signature is the existence of a

relatively light Higgsino together with ~ 35 GeV DM, whose dominant decay modes are

$$\tilde{H}^\pm \rightarrow W^\pm \tilde{\chi}_1^0, \quad (30)$$

$$\tilde{H}_{1,2}^0 \rightarrow Z \tilde{\chi}_1^0 / H \tilde{\chi}_1^0. \quad (31)$$

The decay branching ratios are given in Fig. 2. We shall discuss each signature in detail in the following.

A. Dark Matter Production versus Mono-jet

If only one DM pair is produced at a hadron collider, it will not leave any information inside the detector. One way to probe this process is through a hard initial state radiation (ISR) jet, which is recoiling against the DM pair. As result, the signal presents a large unbalanced transverse energy. At the LHC, the CMS Collaboration has carried out a mono-jet search [71] with a data set of 20 fb^{-1} . Their analysis shows that the current stage of the LHC is only sensitive to signals with $p_T(\text{ISR}) > 280, 340, 450$ GeV that have cross section greater than about 100, 30, 10 fb, respectively.

For our process, even though the direct production is relatively large (~ 10 pb) because of the small DM mass, the production rate of the mono-jet signal is quite low. This is because, as has been studied in Ref. [72], the spectrum of the radiated jet mainly depends on the mass scale of the final states. In our case, because the DM mass is very small (~ 35 GeV) the production of an energetic ISR jet is suppressed. From the left panel of Fig. 5, we conclude that the p_T spectrum of the ISR jet drops very quickly and only $\sim 1/10^{-4}$ of the events have $p_T(\text{ISR}) > 250$ GeV. The situation will improve very much in the next run of the LHC at 14 TeV. We show the cross section for the allowed models with different cuts on the leading ISR jet and the corresponding CMS exclusion bounds in the right panel of Fig. 5.

The production cross section drops by about four orders of magnitude after we require the leading ISR to have $p_T > 280$ GeV. So the signal is around two orders of magnitude smaller than the current bound. The sensitivity will not become better for harder cuts on the leading ISR jet. So, we may conclude that it will be very difficult to probe the GCE NMSSM through mono-jet signatures at the LHC, even at the 14 TeV upgraded LHC.

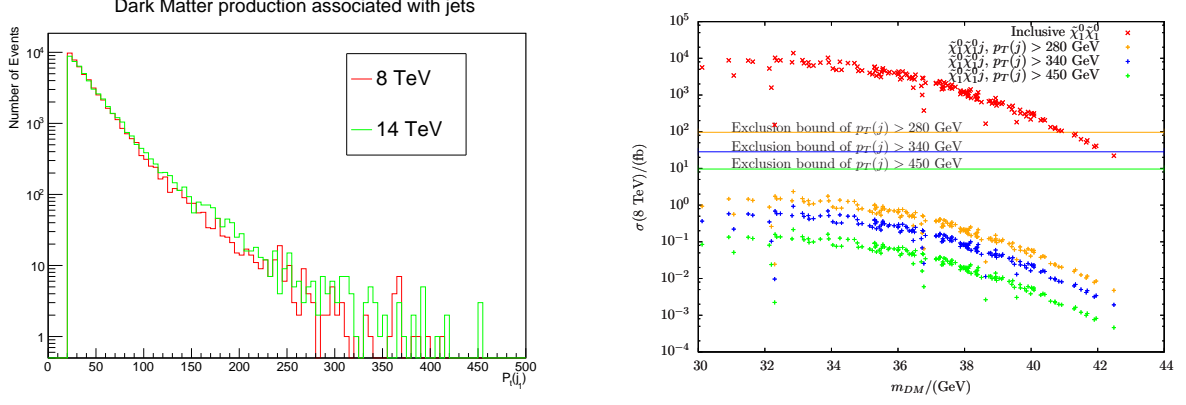


FIG. 5: Left: the p_T spectrum of the leading ISR jet for 35.5 GeV DM pair production at LHC. Right: the cross section in the models for the GCE with corresponding cuts on the leading ISR jet as indicated in the figure. The horizontal lines are the experimental bounds on cross sections for three categories of the models.

B. Searching the Di-Higgs Final State

The detection of Higgs boson pair production is not only important for the potential to reveal new physics but also important for testing the SM itself. A signature of our models is that the Higgs particles can be pair produced by neutral Higgsino pair production with subsequently decay into Higgs and DM with large branching ratios as shown in Fig. 2.

At the LHC, the neutral Higgsino pair is mainly produced through s -channel Z boson exchange. As a result, the production cross section is dominated by the coupling between the Z boson and Higgsino pair

$$Z_\mu \tilde{\chi}_i^0 \tilde{\chi}_j^0 = \frac{ie}{2s_W c_W} \gamma^\mu ((Z_{i4}^* Z_{j4}^* - Z_{i3}^* Z_{j3}^*) P_L + (Z_{j4}^* Z_{i4}^* - Z_{j3}^* Z_{i3}^*) P_R), \quad (32)$$

where N_{ij} is the neutralino mixing matrix. We show the mixing factor $(Z_{i4}^* Z_{j4}^* - Z_{i3}^* Z_{j3}^*)$ for the different combinations in the left panel of Fig. 6. From this figure, we know that in our case, the dominant production of neutral Higgsino pair is $\tilde{\chi}_2^0 \tilde{\chi}_3^0$, *i.e.*, the pair with different masses.

In Ref. [73], the CMS Collaboration has also tried to search for the di-Higgs signal from Higgsino decay. Because there is only a small excess in the observed number of events, a very loose bound is obtained as shown by the red line in the right panel of Fig. 6. The green points in the same figure show the corresponding cross sections of our signal processes. Our models are far beyond the reach of a di-Higgs analysis based on the current data base.

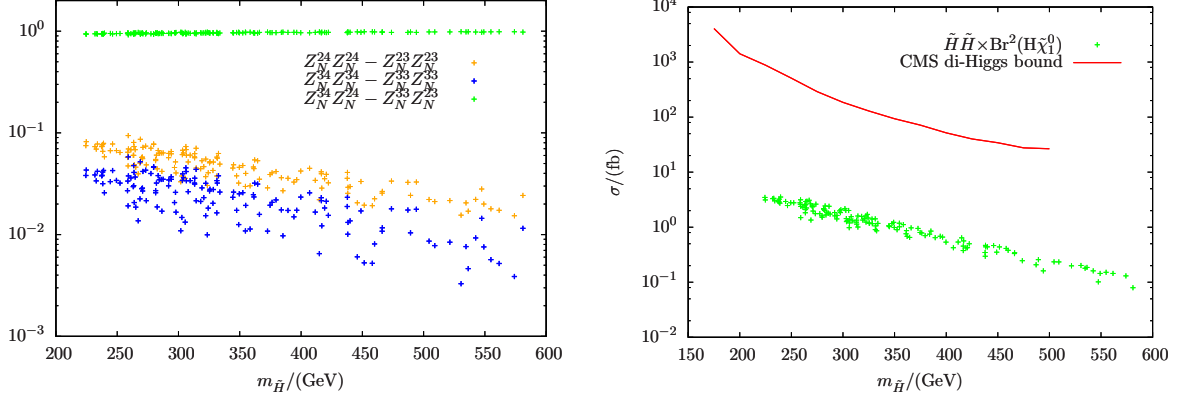


FIG. 6: Left: the mixing factor of Z coupling to each pair of neutral Higgsinos. Right: the cross section for the signal models and exclusion bound by the CMS Collaboration.

C. Electroweakino Searches at 14 TeV LHC

In this subsection, we will study two traditional but much more sensitive channels

$$\tilde{\chi}_{2,3}^0 \tilde{\chi}_1^\pm \rightarrow H_{SM} \tilde{\chi}_1^0 + W^\pm \tilde{\chi}_1^0, \quad (33)$$

$$\tilde{\chi}_{2,3}^0 \tilde{\chi}_1^\pm \rightarrow Z \tilde{\chi}_1^0 + W^\pm \tilde{\chi}_1^0. \quad (34)$$

In fact, these two channels also give rise to the most stringent bounds on Winos at 8 TeV LHC searches. For WH final states [74], the Wino has been excluded for masses up to ~ 300 GeV for $m_{\tilde{\chi}_1^0} \sim 35$ GeV. For WZ final states [75], all Wino masses below 420 GeV for $m_{\tilde{\chi}_1^0} \sim 35$ GeV are excluded. As in our case, the production rates of the chargino and neutralino pairs are suppressed due to the mixing between Higgsino states. Moreover, the required final states are suppressed by their decay branching ratios. Thus, in order to get improved sensitivities to the NMSSM model with GCE, we have to consider the 14 TeV LHC.

1. WH Channel

The ATLAS analysis in Ref. [74], where the W boson decays leptonically while the Higgs boson decays to $b\bar{b}$, gives the strongest bound for the WH channel at the current stage of LHC. Because the ATLAS search had interest in neutralino and chargino mass regions similar to ours, we choose to use those discriminate variables in their paper to separate the signal and backgrounds. We follow their analysis at 8 TeV and attempt to extrapolate to 14 TeV, where some minor changes are applied in order to optimize the search. There have been some other studies [76, 77] of the

WH channel at the 14 TeV LHC, which used similar cuts. However, their results are either based on a specific model or on simplified models and we were unable to directly apply their studies in our analysis. Refs. [78, 79] also studied the WH channel with H decaying to various final states, however the sensitivities of the other final states considered were not much improved compared to the dominant $b\bar{b}l^\pm + E_T^{\text{miss}}$ because of their suppressed branching ratios. A very recent ATLAS analysis [80] considered the $\gamma\gamma l$ and same-sign di-lepton final states as well. Their results showed that the strongest expected exclusion limit for heavy electroweakino region (~ 200 GeV) is from $b\bar{b}l^\pm$ final states. Here, our cuts are chosen as below:

- Exactly one lepton with $p_T > 25$ GeV;
- There should be no more than 3 jets in the event;
- The leading two jets should be b -tagged and their invariant mass is in the range [105, 135] GeV. Furthermore, the contranverse mass of the two b -jets

$$m_{\text{CT}}^2 = (E_T^{b1} + E_T^{b2})^2 - |\mathbf{p}_T^{b1} - \mathbf{p}_T^{b2}|^2 \quad (35)$$

is larger than 160 GeV;

- To remove the W + jets background, the transverse mass of the lepton and missing transverse momentum

$$m_T = \sqrt{2p_T^{\text{lep}} E_T^{\text{miss}} - 2\mathbf{p}_T^{\text{lep}} \cdot \mathbf{p}_T^{\text{miss}}} \quad (36)$$

is required to be larger than 130 GeV since our Higgsinos tend to be heavier than 200 GeV; and

- We define two signal regions SRA and SRB for different masses of Higgsino which correspond to $E_T^{\text{miss}} > 100$ and $E_T^{\text{miss}} > 245$, respectively. We find that the SRB is more sensitive for Higgsino mass greater than 300 GeV.

The dominant backgrounds for our analyses are $t\bar{t}$, single top, and $Wb\bar{b}$. We generate those backgrounds by MadGraph5 [81], where Pythia6 [82] and Delphes 3.1.2 [83] have been used to implement parton shower and detector simulation. The $t\bar{t}$ is generated up to two additional jets, where the MLM matching adopted in MadGraph5 is used to avoid double counting between matrix element and parton shower. All three single top production modes (t -channel, s -channel and tW process) are considered in our generation. We use the default ATLAS setup for detector simulation. Their cross sections before and after the cuts for both signal regions are shown in Table IV.

	$\sigma(14 \text{ TeV})/\text{pb}$	SRA/fb	SRB/fb
$t\bar{t}$	877.2	0.39	2.3×10^{-2}
single top	318.5	0.064	3.2×10^{-3}
$Wb\bar{b}$	128	0.0096	6.4×10^{-4}

TABLE IV: The background cross sections before and after the cuts for each signal region.

As for the cut efficiency of signal processes ϵ_s , because we have DM mass ~ 35 GeV and Higgsino mass in the range $[200, 600]$ GeV, we generate the process of $\tilde{\chi}_2^0 \tilde{\chi}_1^\pm$ pair production with subsequent decays $\tilde{\chi}_1^\pm \rightarrow W^\pm \tilde{\chi}_1^0$ and $\tilde{\chi}_2^0 \rightarrow H_{\text{SM}} \tilde{\chi}_1^0$ in Madgraph5 as well. The step size for Higgsino mass is chosen as 20 GeV.

After obtaining the cut efficiency for the signal events, we can estimate the exclusion bound according to

$$\sigma \sim \frac{S}{\sqrt{B}} = \frac{\sigma_s \epsilon_s}{\sqrt{\sigma_b \epsilon_b}} \times \sqrt{\mathcal{L}}, \quad (37)$$

where $\sigma_b \epsilon_b$ is given in Table IV and \mathcal{L} is the luminosity. The corresponding 3- σ exclusion limit for the WH final state is shown as red curve in the left panel of Fig. 7.

The production cross section of the signal process for each of our NMSSM models is calculated by passing the SLHA [84] output that is generated from NMSSMtools into Madgraph5. We assume a K-factor of 1.2 for all those models.

Taking the resulting cross sections of the signal processes, we project our models to the exclusion plane that we have obtained before. The results are given in Fig. 7 from which we conclude that only a small amount of our models can be detected at 14 TeV LHC with luminosity 3000 fb^{-1} . The relatively weak exclusion limit is mainly because of the low cut efficiency of the signal events. We find the reduction of efficiency is dominated by the requirement of “exactly two b-jets and one lepton in the final state”, which reduces the number of signal events by about 2 order of magnitude. This can be roughly estimated by $\text{Br}(W \rightarrow l\nu) \times \text{Br}(h \rightarrow b\bar{b}) \times \epsilon_{b \text{ tag}}^2 \sim 5 \times 10^{-2}$. In a realistic detector, the efficiency turns out to be further suppressed. Furthermore, relatively strong cuts are imposed on missing transverse energy ($E_T^{\text{miss}} > 245$ GeV), contranverse mass ($M_{\text{CT}} > 160$ GeV) and transverse mass ($M_T > 130$ GeV) in order to suppress the Z +jets/diboson, $t\bar{t}$ and W backgrounds respectively. As a result, each of these cuts removes more than half of the events.

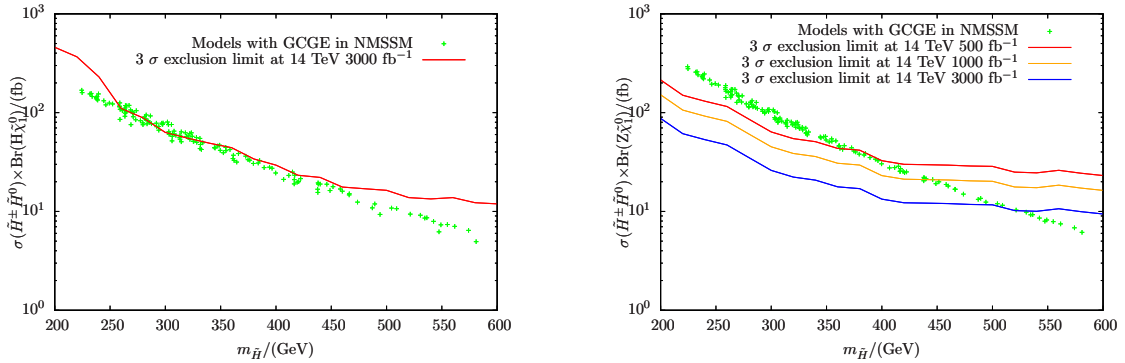


FIG. 7: Left: the production cross section of WH final states and its corresponding exclusion limit at 14 TeV LHC with luminosity 3000 fb^{-1} . Right: the production cross sections of WZ final states and their corresponding exclusion limits at 14 TeV LHC with luminosities 500 fb^{-1} , 1000 fb^{-1} and 3000 fb^{-1} , respectively.

2. WZ Channel

The searches for both 3-lepton final states [52, 85] and 2-lepton + jets [75] give very strong bound on these decay modes of chargino and neutralino pair productions. The current bound is actually given by the combination of these two searches. Even though the tri-lepton search is more sensitive to lighter chargino and neutralino region, the 2-lepton + jets is slightly better at higher mass region. Thus, in this subsection, we will re-produce the SR- Z jets analysis in Ref. [75] and extrapolate it to 14 TeV LHC with a few optimizations. The cuts chosen by ATLAS Collaboration are listed as follows:

- Exact two opposite sign same flavor (OSSF) leptons are required. Also, these two leptons should have $p_T(l_1) > 35 \text{ GeV}$ and $p_T(l_2) > 20 \text{ GeV}$, respectively;
- Because the OSSF lepton pair is from a moderately boosted Z boson decay, two additional cuts on leptons are imposed: $81.2 \text{ GeV} < m_{ll} < 101.2 \text{ GeV}$, and $p_T(ll) > 80 \text{ GeV}$. In addition, the angular separation between two leptons must satisfy $0.3 < \Delta R(ll) < 1.5$;
- There should be no b -jet, τ -jet and forward jet in the event;
- The two highest- p_T central jets must have $p_T > 45 \text{ GeV}$. They are expected from W boson decay and then satisfy the invariant mass range $50 \text{ GeV} < m_{jj} < 100 \text{ GeV}$; and

- A cut on $E_T^{\text{miss,rel}}$ is applied: $E_T^{\text{miss,rel}} > 80$ GeV, where

$$E_T^{\text{miss,rel}} = \begin{cases} E_T^{\text{miss}} & , \text{ if } \Delta\phi_{l,j} \geq \pi/2 \\ E_T^{\text{miss}} \times \Delta\phi_{l,j} & , \text{ if } \Delta\phi_{l,j} < \pi/2 \end{cases}, \quad (38)$$

where $\Delta\phi$ is the azimuthal angle between the direction of $\mathbf{p}_T^{\text{miss}}$ and that of the nearest lepton or jet.

The dominant backgrounds are the leptonic decay of $W^\pm W^\mp$, the leptonic decay of $W^\pm Z$ where the lepton from W decay is not reconstructed, and ZZ with one of the Z bosons decaying into charged leptons while the other decays into neutrinos. All those backgrounds are generated with up to two additional jets by Madgraph5 using a procedure similar to that described above. In this case, the cross section before and after the cuts are given in Table V.

	$\sigma(14 \text{ TeV})/\text{pb}$	SR/fb
$W^\pm W^\mp + \text{jets}$	124.3	0.029
$W^+ Z + \text{jets}$	31.5	0.028
$W^- Z + \text{jets}$	20.32	0.012
$ZZ + \text{jets}$	17.72	0.13

TABLE V: The background cross sections before and after the cuts for WZ final state.

The signal process for the WZ final state is generated similarly to what was done for the WH process. The expected $3\text{-}\sigma$ exclusion limits for 14 TeV LHC with luminosities 500 fb^{-1} , 1000 fb^{-1} , and 3000 fb^{-1} are given in the right panel of Fig. 7. From the figure, we find the sensitivity for the WZ channel is much better than that for the WH channel, especially in the low mass region of the Higgsino. At 14 TeV with 500 fb^{-1} from the LHC, the NMSSM models with Higgsino lighter than ~ 370 GeV may be excluded.

V. CONCLUSION

We have discussed possible scenarios in the NMSSM with a discrete Z_3 symmetry that may be able to explain the Galactic Centre Excess (GCE). It turns out that the s -channel A_1 resonant annihilation into $b\bar{b}$, is the most promising scenario for realization of the the gamma-ray excess. In this scenario, even though the GCE is produced by the A_1 resonant annihilation, the DM annihilation at freeze-out is mainly contributed to by the s -channel Z boson exchange process. In order to get the correct DM relic density, the coupling between the Z boson and DM is enhanced

by a relatively large Higgsino component in the DM and large $\tan\beta$. We also briefly comment on the hidden sector dark matter scenario, in which DM is annihilating into a singlet Higgs pair. The subsequent decays of these Higgs bosons into b quarks are able to produce the observed GCE signal. However, in the NMSSM each of the DM mass, the DM coupling with Higgs bosons, and the Higgsino mass are highly correlated. We need a relatively large singlino dominant DM mass of ~ 76 GeV and a larger superpotential coupling κ to successfully reproduce the GCE signal. As a result, the DM annihilation cross section is bounded from above by DM direct detection. So, the GCE can only be approximately fitted in hidden sector DM scenario.

The s -channel A_1 resonant process is the most promising channel to explain the GCE in the NMSSM. We have studied its LHC phenomenology for the parameter space consistent with an explanation of the GCE. For this purpose we have considered the discovery potential of four promising signatures in detail. Firstly, we considered DM pair production which recoils against a hard initial state radiation (ISR) jet. Because the energy spectrum of the ISR jet is suppressed by the small DM mass, the production rate of the required signal event is two orders of magnitude smaller than currently available sensitivity. The situation will not become significantly better for the next higher-energy phase of the LHC. Secondly, we considered the pair production of neutral Higgsinos that subsequently decay into a Higgs pair. This channel, despite its interesting features, is two orders of magnitude smaller than current sensitivity as well. Thirdly, we considered two traditional channels which consist of chargino and neutralino pair production with subsequent decays into WH +DMs and WZ +DMs, respectively. By extrapolating the two most sensitive analyses of the ATLAS Collaboration, we found that for the LHC with 14 TeV energy: (a) for the WH channel part of the model space for the first scenario is discoverable with an integrated luminosity of 3000 fb^{-1} ; and (b) for the WZ channel most of the model space is discoverable and only requires 500 fb^{-1} of integrated luminosity.

Acknowledgements

We would like to thank Yandong Liu for collaboration at the early stage of the work. This research was supported in part by the Australian Research Council through Grant No. CE110001004 (CoEPP) and by the University of Adelaide (JL and AGW), as well as by the Natural Science Foundation of China under grant numbers 10821504, 11075194, 11135003, 11275246, and

11475238, and by the National Basic Research Program of China (973 Program) under grant number 2010CB833000 (JG and TL).

A. NEUTRALINO AND HIGGS MASS MATRICES

We use the convention in Ref. [37]

$$\tan\beta = \frac{v_u}{v_d}, \quad (39)$$

$$\mu_{\text{eff}} = \lambda v_s, \quad (40)$$

$$M_A^2 = \frac{2\lambda v_s}{\sin 2\beta} (A_\lambda + \kappa v_s), \quad (41)$$

$$v = \sqrt{v_u^2 + v_d^2} = 174 \text{ GeV}, \quad (42)$$

where v_d , v_u , and s are the VEVs of H_d , H_u , and S , respectively. The symmetric neutralino mass matrix in the $(\tilde{B}, \tilde{W}, \tilde{H}_d, \tilde{H}_u, \tilde{S})$ basis can be written as follows

$$\mathcal{M}_0 = \begin{pmatrix} M_1 & 0 & -\frac{g_1 v_d}{\sqrt{2}} & \frac{g_1 v_u}{\sqrt{2}} & 0 \\ & M_2 & \frac{g_2 v_d}{\sqrt{2}} & -\frac{g_2 v_u}{\sqrt{2}} & 0 \\ & & 0 & -\mu_{\text{eff}} & -\lambda v_u \\ & & & 0 & -\lambda v_d \\ & & & & 2\kappa s \end{pmatrix}. \quad (43)$$

The lightest neutralino is the mixing of gauge eigenstates

$$\tilde{\chi}_1^0 = N_{11}\tilde{B} + N_{12}\tilde{W} + N_{13}\tilde{H}_u + N_{14}\tilde{H}_d + N_{15}\tilde{S}, \quad (44)$$

and its mass approximately is $m_{\tilde{\chi}_1^0} \sim 2\kappa s$ if it is singlino-like. In the $2\kappa/\lambda \ll 1$ limit, the Higgsino components of the $\tilde{\chi}_1^0$ can be estimated as below [22]

$$\frac{N_{13}}{N_{15}} = \frac{\lambda v}{\mu^2 - m_{\tilde{\chi}_1^0}^2} c_\beta (t_\beta m_{\tilde{\chi}_1^0} - \mu), \quad (45)$$

$$\frac{N_{14}}{N_{15}} = \frac{-\lambda v}{\mu^2 - m_{\tilde{\chi}_1^0}^2} s_\beta \left(\mu - \frac{m_{\tilde{\chi}_1^0}}{t_\beta} \right), \quad (46)$$

where we have used c_β , s_β , and t_β for $\cos\beta$, $\sin\beta$, and $\tan\beta$, respectively.

The 3×3 symmetric CP-even Higgs boson mass matrix in the (S_1, S_2, S_3) basis [56] is

$$\mathcal{M}_S^2 = \begin{pmatrix} M_A^2 + s_{2\beta}^2(m_Z^2 - \lambda^2 v^2) & s_{2\beta}c_{2\beta}(m_Z^2 - \lambda^2 v^2) & -\lambda v c_{2\beta}(A_\lambda + \frac{2\kappa\mu}{\lambda}) \\ & c_{2\beta}^2 m_Z^2 + \lambda^2 v^2 s_{2\beta}^2 & 2\lambda v(\mu - s_\beta c_\beta(A_\lambda + \frac{2\kappa\mu}{\lambda})) \\ & & \frac{s_{2\beta}}{2} \frac{\lambda^2 v^2}{\mu} A_\lambda + \frac{\kappa\mu}{\lambda} (A_\kappa + 4\frac{\kappa\mu}{\lambda}) \end{pmatrix}. \quad (47)$$

In the case of very light singlet, the singlet component of the SM Higgs H_{SM} can be suppressed by requiring

$$(\mathcal{M}_S^2)_{23} \simeq 0. \quad (48)$$

The Eq. (48) can be used to determine the approximation value of A_λ as follows

$$A_\lambda \simeq \frac{2\mu}{s_{2\beta}} - \frac{2\kappa\mu}{\lambda}. \quad (49)$$

Finally, we give the simplest 2×2 symmetric CP-odd Higgs mass matrix in the (P_1, P_2) basis

$$\mathcal{M}_P^2 = \begin{pmatrix} M_A^2 & \lambda v(A_\lambda - 2\frac{\kappa\mu}{\lambda}) \\ -\frac{3\kappa\mu A_\kappa}{\lambda} + \frac{\lambda^2 v^2}{2\mu} s_{2\beta}(A_\lambda + \frac{4\kappa\mu}{\lambda}) & \end{pmatrix}. \quad (50)$$

-
- [1] **LUX Collaboration** Collaboration, D. Akerib *et al.*, “First results from the LUX dark matter experiment at the Sanford Underground Research Facility,” *Phys.Rev.Lett.* **112** (2014) 091303, 1310.8214.
 - [2] **SuperCDMS Collaboration** Collaboration, R. Agnese *et al.*, “Search for Low-Mass WIMPs with SuperCDMS,” *Phys.Rev.Lett.* **112** (2014) 241302, 1402.7137.
 - [3] T. Daylan, D. P. Finkbeiner, D. Hooper, T. Linden, S. K. N. Portillo, *et al.*, “The Characterization of the Gamma-Ray Signal from the Central Milky Way: A Compelling Case for Annihilating Dark Matter,” 1402.6703.
 - [4] A. Alves, S. Profumo, F. S. Queiroz, and W. Shepherd, “The Effective Hooperon,” 1403.5027.
 - [5] A. Berlin, D. Hooper, and S. D. McDermott, “Simplified Dark Matter Models for the Galactic Center Gamma-Ray Excess,” *Phys.Rev.* **D89** (2014) 115022, 1404.0022.
 - [6] P. Agrawal, B. Batell, D. Hooper, and T. Lin, “Flavored Dark Matter and the Galactic Center Gamma-Ray Excess,” 1404.1373.
 - [7] E. Izaguirre, G. Krnjaic, and B. Shuve, “The Galactic Center Excess from the Bottom Up,” *Phys.Rev.* **D90** (2014) 055002, 1404.2018.
 - [8] S. Ipek, D. McKeen, and A. E. Nelson, “A Renormalizable Model for the Galactic Center Gamma Ray Excess from Dark Matter Annihilation,” 1404.3716.
 - [9] P. Ko, W.-I. Park, and Y. Tang, “Higgs portal vector dark matter for GeV scale γ -ray excess from galactic center,” 1404.5257.
 - [10] M. Abdullah, A. DiFranzo, A. Rajaraman, T. M. Tait, P. Tanedo, *et al.*, “Hidden On-Shell Mediators for the Galactic Center Gamma-Ray Excess,” *Phys.Rev.* **D90** (2014) 035004, 1404.6528.
 - [11] A. Martin, J. Shelton, and J. Unwin, “Fitting the Galactic Center Gamma-Ray Excess with Cascade Annihilations,” 1405.0272.

- [12] A. Berlin, P. Gratia, D. Hooper, and S. D. McDermott, “Hidden Sector Dark Matter Models for the Galactic Center Gamma-Ray Excess,” *Phys.Rev.* **D90** (2014) 015032, 1405.5204.
- [13] J. M. Cline, G. Dupuis, Z. Liu, and W. Xue, “The windows for kinetically mixed Z' -mediated dark matter and the galactic center gamma ray excess,” *JHEP* **1408** (2014) 131, 1405.7691.
- [14] D. K. Ghosh, S. Mondal, and I. Saha, “Confronting the Galactic Center Gamma Ray Excess With a Light Scalar Dark Matter,” 1405.0206.
- [15] C. Boehm, M. J. Dolan, and C. McCabe, “A weighty interpretation of the Galactic Centre excess,” *Phys.Rev.* **D90** (2014) 023531, 1404.4977.
- [16] L. Wang, “A simplified 2HDM with a scalar dark matter and the galactic center gamma-ray excess,” 1406.3598.
- [17] P. Agrawal, M. Blanke, and K. Gemmler, “Flavored dark matter beyond Minimal Flavor Violation,” 1405.6709.
- [18] T. Han, Z. Liu, and S. Su, “Light Neutralino Dark Matter: Direct/Indirect Detection and Collider Searches,” *JHEP* **1408** (2014) 093, 1406.1181.
- [19] J. Huang, T. Liu, L.-T. Wang, and F. Yu, “Supersymmetric Sub-Electroweak Scale Dark Matter, the Galactic Center Gamma-ray Excess, and Exotic Decays of the 125 GeV Higgs Boson,” 1407.0038.
- [20] C. Balzs and T. Li, “Simplified Dark Matter Models Confront the Gamma Ray Excess,” 1407.0174.
- [21] B. D. Fields, S. L. Shapiro, and J. Shelton, “Galactic Center Gamma-Ray Excess from Dark Matter Annihilation: Is There A Black Hole Spike?,” 1406.4856.
- [22] C. Cheung, M. Papucci, D. Sanford, N. R. Shah, and K. M. Zurek, “NMSSM Interpretation of the Galactic Center Excess,” 1406.6372.
- [23] K. Kong and J.-C. Park, “Bounds on Dark Matter Interpretation of Fermi-LAT GeV Excess,” 1404.3741.
- [24] T. Bringmann, M. Vollmann, and C. Weniger, “Updated cosmic-ray and radio constraints on light dark matter: Implications for the GeV gamma-ray excess at the Galactic center,” 1406.6027.
- [25] M. Cirelli, D. Gaggero, G. Giesen, M. Taoso, and A. Urbano, “Antiproton constraints on the GeV gamma-ray excess: a comprehensive analysis,” 1407.2173.
- [26] N. Okada and O. Seto, “Galactic center gamma ray excess from two Higgs doublet portal dark matter,” 1408.2583.
- [27] D. Borah and A. Dasgupta, “Galactic Center Gamma Ray Excess in a Radiative Neutrino Mass Model,” 1409.1406.
- [28] M. Cahill-Rowley, J. Gainer, J. Hewett, and T. Rizzo, “Towards a Supersymmetric Description of the Fermi Galactic Center Excess,” 1409.1573.
- [29] C. Arina, E. Del Nobile, and P. Panci, “Not so Coy Dark Matter explains DAMA (and the Galactic Center excess),” 1406.5542.
- [30] E. Hardy, R. Lasenby, and J. Unwin, “Annihilation Signals from Asymmetric Dark Matter,” *JHEP* **1407** (2014) 049, 1402.4500.

- [31] A. D. Banik and D. Majumdar, “Low Energy Gamma Ray Excess Confronting a Singlet Scalar Extended Inert Doublet Dark Matter Model,” 1408.5795.
- [32] C. Boehm, M. J. Dolan, C. McCabe, M. Spannowsky, and C. J. Wallace, “Extended gamma-ray emission from Coy Dark Matter,” *JCAP* **1405** (2014) 009, 1401.6458.
- [33] N. F. Bell, S. Horiuchi, and I. M. Shoemaker, “Annihilating Asymmetric Dark Matter,” 1408.5142.
- [34] K. P. Modak, D. Majumdar, and S. Rakshit, “A Possible Explanation of Low Energy γ -ray Excess from Galactic Centre and Fermi Bubble by a Dark Matter Model with Two Real Scalars,” 1312.7488.
- [35] **ATLAS Collaboration** Collaboration, G. Aad *et al.*, “Observation of a new particle in the search for the Standard Model Higgs boson with the ATLAS detector at the LHC,” *Phys.Lett.* **B716** (2012) 1–29, 1207.7214.
- [36] **CMS Collaboration** Collaboration, S. Chatrchyan *et al.*, “Observation of a new boson at a mass of 125 GeV with the CMS experiment at the LHC,” *Phys.Lett.* **B716** (2012) 30–61, 1207.7235.
- [37] U. Ellwanger, C. Hugonie, and A. M. Teixeira, “The Next-to-Minimal Supersymmetric Standard Model,” *Phys.Rept.* **496** (2010) 1–77, 0910.1785.
- [38] U. Ellwanger, G. Espitalier-Noel, and C. Hugonie, “Naturalness and Fine Tuning in the NMSSM: Implications of Early LHC Results,” *JHEP* **1109** (2011) 105, 1107.2472.
- [39] G. G. Ross and K. Schmidt-Hoberg, “The Fine-Tuning of the Generalised NMSSM,” *Nucl.Phys.* **B862** (2012) 710–719, 1108.1284.
- [40] L. J. Hall, D. Pinner, and J. T. Ruderman, “A Natural SUSY Higgs Near 126 GeV,” *JHEP* **1204** (2012) 131, 1112.2703.
- [41] Z. Kang, J. Li, and T. Li, “On Naturalness of the MSSM and NMSSM,” *JHEP* **1211** (2012) 024, 1201.5305.
- [42] J.-J. Cao, Z.-X. Heng, J. M. Yang, Y.-M. Zhang, and J.-Y. Zhu, “A SM-like Higgs near 125 GeV in low energy SUSY: a comparative study for MSSM and NMSSM,” *JHEP* **1203** (2012) 086, 1202.5821.
- [43] J. Cao, Z. Heng, J. M. Yang, and J. Zhu, “Status of low energy SUSY models confronted with the LHC 125 GeV Higgs data,” *JHEP* **1210** (2012) 079, 1207.3698.
- [44] J. R. Espinosa, C. Grojean, V. Sanz, and M. Trott, “NSUSY fits,” *JHEP* **1212** (2012) 077, 1207.7355.
- [45] M. Perelstein and B. Shakya, “XENON100 implications for naturalness in the MSSM, NMSSM, and lambda-supersymmetry model,” *Phys.Rev.* **D88** (2013), no. 7, 075003, 1208.0833.
- [46] K. Agashe, Y. Cui, and R. Franceschini, “Natural Islands for a 125 GeV Higgs in the scale-invariant NMSSM,” *JHEP* **1302** (2013) 031, 1209.2115.
- [47] S. King, M. Muhlleitner, and R. Nevzorov, “NMSSM Higgs Benchmarks Near 125 GeV,” *Nucl.Phys.* **B860** (2012) 207–244, 1201.2671.
- [48] S. King, M. Mhlleitner, R. Nevzorov, and K. Walz, “Natural NMSSM Higgs Bosons,” *Nucl.Phys.* **B870** (2013) 323–352, 1211.5074.
- [49] T. Gherghetta, B. von Harling, A. D. Medina, M. A. Schmidt, and T. Trott, “SUSY Implications

- from WIMP Annihilation into Scalars at the Galactic Centre,” 1502.07173.
- [50] D. Cerdeo, M. Peir, and S. Robles, “Low-mass right-handed sneutrino dark matter: SuperCDMS and LUX constraints and the Galactic Centre gamma-ray excess,” *JCAP* **1408** (2014) 005, 1404.2572.
 - [51] D. Cerdeno, M. Peiro, and S. Robles, “Fits to the Fermi-LAT GeV excess with RH sneutrino dark matter: implications for direct and indirect dark matter searches and the LHC,” 1501.01296.
 - [52] **ATLAS Collaboration** Collaboration, G. Aad *et al.*, “Search for direct production of charginos and neutralinos in events with three leptons and missing transverse momentum in $\sqrt{s} = 8\text{TeV}$ pp collisions with the ATLAS detector,” *JHEP* **1404** (2014) 169, 1402.7029.
 - [53] J. F. Navarro, A. Ludlow, V. Springel, J. Wang, M. Vogelsberger, *et al.*, “The Diversity and Similarity of Cold Dark Matter Halos,” 0810.1522.
 - [54] J. Diemand, M. Kuhlen, P. Madau, M. Zemp, B. Moore, *et al.*, “Clumps and streams in the local dark matter distribution,” *Nature* **454** (2008) 735–738, 0805.1244.
 - [55] **Planck Collaboration** Collaboration, P. Ade *et al.*, “Planck 2013 results. XVI. Cosmological parameters,” *Astron.Astrophys.* (2014) 1303.5076.
 - [56] D. Miller, R. Nevzorov, and P. Zerwas, “The Higgs sector of the next-to-minimal supersymmetric standard model,” *Nucl.Phys.* **B681** (2004) 3–30, hep-ph/0304049.
 - [57] J. Kumar and D. Marfatia, “Matrix element analyses of dark matter scattering and annihilation,” *Phys.Rev.* **D88** (2013), no. 1, 014035, 1305.1611.
 - [58] LEP SUSY Working Group, ALEPH, DELPHI, L3 and OPAL experiments, “Combined LEP chargino results, up to 208 GeV for large m_0 “ LEPSUSYWG/01-03.1.
 - [59] G. Jungman, M. Kamionkowski, and K. Griest, “Supersymmetric dark matter,” *Phys.Rept.* **267** (1996) 195–373, hep-ph/9506380.
 - [60] **ATLAS Collaboration** Collaboration, G. Aad *et al.*, “Search for Invisible Decays of a Higgs Boson Produced in Association with a Z Boson in ATLAS,” *Phys.Rev.Lett.* **112** (2014) 201802, 1402.3244.
 - [61] U. Ellwanger, J. F. Gunion, and C. Hugonie, “NMHDECAY: A Fortran code for the Higgs masses, couplings and decay widths in the NMSSM,” *JHEP* **0502** (2005) 066, hep-ph/0406215.
 - [62] U. Ellwanger and C. Hugonie, “NMHDECAY 2.0: An Updated program for sparticle masses, Higgs masses, couplings and decay widths in the NMSSM,” *Comput.Phys.Commun.* **175** (2006) 290–303, hep-ph/0508022.
 - [63] G. Belanger, F. Boudjema, C. Hugonie, A. Pukhov, and A. Semenov, “Relic density of dark matter in the NMSSM,” *JCAP* **0509** (2005) 001, hep-ph/0505142.
 - [64] G. Belanger, F. Boudjema, A. Pukhov, and A. Semenov, “micrOMEGAs.3: A program for calculating dark matter observables,” *Comput.Phys.Commun.* **185** (2014) 960–985, 1305.0237.
 - [65] G. Belanger, F. Boudjema, P. Brun, A. Pukhov, S. Rosier-Lees, *et al.*, “Indirect search for dark matter with micrOMEGAs2.4,” *Comput.Phys.Commun.* **182** (2011) 842–856, 1004.1092.
 - [66] G. Belanger, F. Boudjema, A. Pukhov, and A. Semenov, “Dark matter direct detection rate in a generic model with micrOMEGAs 2.2,” *Comput.Phys.Commun.* **180** (2009) 747–767, 0803.2360.

- [67] J. M. Cline, K. Kainulainen, P. Scott, and C. Weniger, “Update on scalar singlet dark matter,” *Phys.Rev.* **D88** (2013) 055025, 1306.4710.
- [68] P. Agrawal, B. Batell, P. J. Fox, and R. Harnik, “WIMPs at the Galactic Center,” 1411.2592.
- [69] F. Calore, I. Cholis, C. McCabe, and C. Weniger, “A Tale of Tails: Dark Matter Interpretations of the Fermi GeV Excess in Light of Background Model Systematics,” 1411.4647.
- [70] M. E. Peskin, “Comparison of LHC and ILC Capabilities for Higgs Boson Coupling Measurements,” 1207.2516.
- [71] **ATLAS Collaboration** Collaboration, G. Aad *et al.*, “Search for pair-produced third-generation squarks decaying via charm quarks or in compressed supersymmetric scenarios in pp collisions at $\sqrt{s}=8$ TeV with the ATLAS detector,” 1407.0608.
- [72] J. Alwall, S. de Visscher, and F. Maltoni, “QCD radiation in the production of heavy colored particles at the LHC,” *JHEP* **0902** (2009) 017, 0810.5350.
- [73] CMS Collaboration [CMS Collaboration], “Search for electroweak production of higgsinos in channels with two Higgs bosons decaying to b quarks in pp collisions at 8 TeV,” CMS-PAS-SUS-13-022.
- [74] The ATLAS collaboration, “Search for chargino and neutralino production in final states with one lepton, two b-jets consistent with a Higgs boson, and missing transverse momentum with the ATLAS detector in 20.3 fb^{-1} of $\sqrt{s} = 8$ TeV pp collisions,” ATLAS-CONF-2013-093, ATLAS-COM-CONF-2013-102.
- [75] **ATLAS Collaboration** Collaboration, G. Aad *et al.*, “Search for direct production of charginos, neutralinos and sleptons in final states with two leptons and missing transverse momentum in pp collisions at $\sqrt{s} = 8$ TeV with the ATLAS detector,” *JHEP* **1405** (2014) 071, 1403.5294.
- [76] H. Baer, V. Barger, A. Lessa, W. Sreethawong, and X. Tata, “Wh plus missing- E_T signature from gaugino pair production at the LHC,” *Phys.Rev.* **D85** (2012) 055022, 1201.2949.
- [77] D. Ghosh, M. Guchait, and D. Sengupta, “Higgs Signal in Chargino-Neutralino Production at the LHC,” *Eur.Phys.J.* **C72** (2012) 2141, 1202.4937.
- [78] T. Han, S. Padhi, and S. Su, “Electroweakinos in the Light of the Higgs Boson,” *Phys.Rev.* **D88** (2013) 115010, 1309.5966.
- [79] A. Papaefstathiou, K. Sakurai, and M. Takeuchi, “Higgs boson to di-tau channel in Chargino-Neutralino searches at the LHC,” *JHEP* **1408** (2014) 176, 1404.1077.
- [80] G. Aad *et al.* [ATLAS Collaboration], “Search for direct pair production of a chargino and a neutralino decaying to the 125 GeV Higgs boson in $\sqrt{s} = 8$ TeV pp collisions with the ATLAS detector,” arXiv:1501.07110 [hep-ex].
- [81] J. Alwall, M. Herquet, F. Maltoni, O. Mattelaer, and T. Stelzer, “MadGraph 5 : Going Beyond,” *JHEP* **1106** (2011) 128, 1106.0522.
- [82] T. Sjostrand, S. Mrenna, and P. Z. Skands, “PYTHIA 6.4 Physics and Manual,” *JHEP* **0605** (2006) 026, hep-ph/0603175.
- [83] **DELPHES 3** Collaboration, J. de Favereau *et al.*, “DELPHES 3, A modular framework for fast

- simulation of a generic collider experiment,” *JHEP* **1402** (2014) 057, 1307.6346.
- [84] B. Allanach, C. Balazs, G. Belanger, M. Bernhardt, F. Boudjema, *et al.*, “SUSY Les Houches Accord 2,” *Comput.Phys.Commun.* **180** (2009) 8–25, 0801.0045.
 - [85] H. Baer, V. Barger, S. Kraml, A. Lessa, W. Sreethawong, *et al.*, “WZ plus missing- E_T signal from gaugino pair production at LHC7,” *JHEP* **1203** (2012) 092, 1201.5382.
 - [86] J. Cao, L. Shang, P. Wu, J. M. Yang, and Y. Zhang, “Supersymmetry explanation of the Fermi Galactic Center excess and its test at LHC run II,” *Phys.Rev.* **D91** (2015), no. 5, 055005, 1410.3239.
 - [87] X.-J. Bi, L. Bian, W. Huang, J. Shu, and P.-F. Yin, “The interpretation for Galactic Center Excess and Electroweak Phase Transition in the NMSSM,” 1503.03749.
 - [88] Several papers [49, 86, 87] following the submission of our work have also used this mechanism to produce the GCE.
 - [89] Ref. [22] showed that DM can also be admixture of Bino and Higgsino. As we will discuss it briefly later, the Bino and Higgsino mixing scenario is similar to the singlino and Higgsino mixing scenario in many aspects.